A perspective on MXenes: Their synthesis, properties, and recent applications

Papadopoulou, K. A., Chroneos, A., Parfitt, D. &

Christopoulos, S. R. G.

Author post-print (accepted) deposited by Coventry University's Repository

Original citation & hyperlink:
Papadopoulou, KA, Chroneos, A, Parfitt, D & Christopoulos, SRG 2020, 'A perspective on MXenes: Their synthesis, properties, and recent applications', Journal of Applied Physics, vol. 128, 170902.
https://dx.doi.org/10.1063/5.0021485

DOI 10.1063/5.0021485
ISSN 0021-8979
ESSN 1089-7550

Publisher: American Institute of Physics

Copyright © and Moral Rights are retained by the author(s) and/ or other copyright owners. A copy can be downloaded for personal non-commercial research or study, without prior permission or charge. This item cannot be reproduced or quoted extensively from without first obtaining permission in writing from the copyright holder(s). The content must not be changed in any way or sold commercially in any format or medium without the formal permission of the copyright holders.

This document is the author's post-print version, incorporating any revisions agreed during the peer-review process. Some differences between the published version and this version may remain and you are advised to consult the published version if you wish to cite from it.

A perspective on MXenes: Their synthesis, properties and recent applications

Konstantina A. Papadopoulou,[1] Alexander Chroneos,[1,2] David Parfitt,[1] and Stavros-Richard G. Christopoulos[1,*]

[1] *Faculty of Engineering, Environment and Computing, Coventry University, Priory Street, Coventry, CV1 5FB, United Kingdom*
[2] *Department of Materials, Imperial College London, London SW7 2BP, UK*

Since 2011, after the discovery of new ceramic two-dimensional materials called MXenes, the attention has been focused on their unique properties and various applications, from energy storage to nanomedicine. We present a brief perspective article of the properties of MXenes, alongside the most recent studies regarding their applications on energy, environment, wireless communications and biotechnology. Future needs regarding the current knowledge about MXenes are also discussed in order to fully understand their nature and overcome the challenges that have restricted their use.

Keywords: MXenes, 2D materials, recent applications, properties

I. INTRODUCTION

MXenes are a new type of material that was first discovered in 2011 after chemically etching a MAX phase[1]. The first MXene was discovered[1] when the *A*-layer of a MAX phase was removed leaving behind two-dimensional (2D) flakes with the general formula $M_{n+1}X_nT_x, (n = 1, 2, 3)$, where T stands for a surface termination, more commonly fluorine (F), hydroxyl (OH), or oxygen (O) atoms[2]. MXenes, therefore, are a family of 2D crystalline materials with theoretically infinite lateral dimensions but atomically thin thickness, whose terminations, i.e., the surface atoms, make them exhibit different properties.

The first MXene discovered was the titanium carbide (Ti_3C_2) at Drexel[1]. Since then, the field has grown with studies of MXenes trying to shed light into their properties and applications. Useful in energy storage, electromagnetic shielding, biology and environmental applications like potable water, MXenes are promising candidates for substituting current materials. It is the scope of this paper to provide an overview of the synthesis and applications of MXenes, as well as a description of the latest discoveries in the field. In Section II, methods used for obtaining MXenes from the corresponding MAX phases are described, while Sections III and IV refer to MXenes' properties and some of their most recent applications respectively, discussing their promise regarding energy storage and conversion. Finally, in Section V, we conclude this perspective article with a description of the gaps in the current knowledge, and issues that need to be addressed in order for MXenes to be widely used.

II. METHODS TO OBTAIN MXENES

A MAX phase is a layered structure of carbides and nitrides with the general formula $M_{n+1}AX_n, (n = 1, 2, 3)$, where M is an early transition metal (groups 3-7 in the periodic table), A is an element belonging in the A-group of the periodic table, and X is either carbon (C) or nitrogen (N)[3–5] (see bottom panel of Fig. 1). The most common practice to obtain MXenes is by wet chemical etching of atomic layers from a multi-layered MAX phase, considering that, in a MAX phase, the layer-to-layer bonding is much weaker than the intralayer one. Initially, the MAX phase is soaked in an acid that destroys the bonds between the transition metal and the A element.

Experiments determined[6] that MXenes obtained via wet chemical etching exhibit higher electronic conductivity and have fewer atomic defects. However, the procedure is only useful for carbon-based MXenes as it fails to remove the A-layer from nitride-based MAX phases.

The first etchant used was hydrofluoric acid (HF)[2,7,8], a material which is considered dangerous to the environment. Therefore, the need arose to find different etchants. A safer mixture of hydrochloric acid (HCl) with lithium fluoride (LiF) started being used in 2014[9]. The problem remained though, because HF gases are produced *in situ*[2]. The issue was solved by the development of different methods to bypass the use of HF. These methods are discussed below.

A. Urea Glass Route

Ma et al.[10] in 2015, synthesized Mo_2C and Mo_2N MXenes from the metal precursor $MoCl_5$ using the urea glass route. They added ethanol into the precursor, thus causing its reaction with the alcohol in order to form Mo-orthoesters. Solid urea was then added to the solution and the mixture was stirred until the urea was fully solubilized. The gel-like result was then heated at 800 °C under a N_2 gas flow, and afterwards calcinated. Silvery black powders were obtained.

Ma et al.[10] performed X-ray diffraction (XRD) on the samples, and no other crystalline side phases, e.g. MoO_x, were observed, a fact that meant that the powders had high purity.

B. Chemical Vapor Deposition

Also in 2015, Xu et al.[11], developed a chemical vapour deposition (CVD) process to obtain MXenes, using methane as the source for C, and a Cu foil above a Mo foil as the substrate. They experimented at a temperature above 1085 °C. During CVD, the decomposition of chemicals on the surface of the substrate leads to deposition, from the vapour phase, of films of materials. The high temperature used, allowed the Cu foil to melt so that a Mo-Cu alloy was formed at the liquid Cu/Mo interface. This resulted in Mo atoms diffusing to the surface of the liquid Cu, thus forming Mo_2C crystals after reacting with the C atoms produced by the decomposition of methane. However, the produced material, although it had MXene-like structure, was in fact a 2D transition metal carbide with larger area than the thus far produced nanosheets that reach up to 10 μm[11].

Xu et al.[11] obtained 2D ultrathin α - Mo_2C crystals a few nanometres thick, and with lateral sizes larger than 100 μm. They were able to control the thickness via the concentration of methane used. The resulted MXene-like material was free of defects, and its superconductivity was stable when the material came in contact with air for a few months[11].

C. Molten Salt Etching

The first time the molten salt etching method was used for MXenes was in 2016[12]. Urbankowski et al.[12] mixed Ti_4AlN_3 powder with a fluoride salt mixture in a 1:1 mass ratio and heated the mixture at 550 °C for 30 min. They found five different fluoride phases containing Al, but the absence of Ti-containing fluorides, confirmed the selectivity of etching. To dissolve the Al-containing fluorides, they used diluted sulphuric acid (H_2SO_4) and the etching products were then removed by washing with deionized water and then centrifugation and decanting. The XRD pattern showed that almost all the fluoride salts were removed and that the resulting powder contained $Ti_4N_3T_x$, where T stands for either OH or F surface terminations, and still unetched Ti_4AlN_3. To further decompose the layered $Ti_4N_3T_x$ MXene, the powder was mixed with tetrabutylammonium hydroxide (TBAOH) which was then removed by washing with deionized water and then centrifuged and decanted. Deionized water was added to the remaining powder, which was then probe sonicated and centrifuged. The result was finally filtered and the smaller unlayered $Ti_4N_3T_x$ flakes ($T = OH, F$) were collected.

The resulted MXene showed more atomic defects than the one obtained through HF-etching, which reduce the value of breaking strength of the material.

D. Hydrothermal Synthesis in an aqueous NaOH solution

Li et al.[13] reported in 2018 a method to obtain $Ti_3C_2T_x$ MXene from the Ti_3AlC_2 MAX phase, assisted by sodium hydroxide (NaOH). In this method, the hydroxide anions (OH^-) attack the Al layers, that results in the oxidation of the Al atoms. The Al hydroxides $Al(OH)_4^-$ produced are then dissolved in alkali and the exposed Ti atoms are terminated by OH or O. However, the process allows for new Al hydroxides to be formed that are confined into the lattice from the Ti layers and cannot further react anew with the OH^-. The problem was eliminated with the application of a series of hydrothermal temperatures and concentrations of NaOH water solutions under an argon atmosphere.

The MXenes obtained through this hydrothermal procedure, have more OH and O terminations than their HF-etching counterparts, and this significantly enhances their performance as supercapacitors.

E. Electrochemical Synthesis at Room Temperature

Yang et al.[14] in 2018, first proposed an electrochemical method without the use of F for the delamination of Ti_3C_2 in a binary aqueous electrolyte. They constructed a two-electrode system with bulk Ti_3AlC_2 as anode and cathode. Only the anode underwent the etching process and produced $Ti_3C_2T_x$. To avoid the fact that the etching only takes place on the surface[15] and allow the electrolyte ions to diffuse into the deeper layers of the anode, they used a mix of 1 M NH_4Cl and 0.2 M tetramethylammonium hydroxide (TMAOH) with a $pH > 9$. Applying a low potential of $+5V$, the bulk anode was gradually delaminated. Afterwards, the sediment and suspended powders of $Ti_3C_2T_x$ were ground and transferred into 25% w/w TMAOH in order to get individual sheets of $Ti_3C_2T_x$.

The resulted MXenes exhibited an electrical conductivity similar to that of the ones produced after the use of HF or HCl/LiF[9]. However, the electrochemical method appears to be the most promising one regarding the overall etching yield, as up to 60% of the bulk material can be transformed into $Ti_3C_2T_x$[14].

In Figure 1 we see the Ti_3AlC_2 MAX phase alongside the Ti_3C_2 resulted bare MXene where the Al layers have been removed. In Fig. 2, the terminated Ti_2CT_2 and $Ti_3C_2T_2$ MXenes[16] are showed.

Finally, Fig. 3 shows the timeline of the etching methods used to produce MXenes until 2017[18].

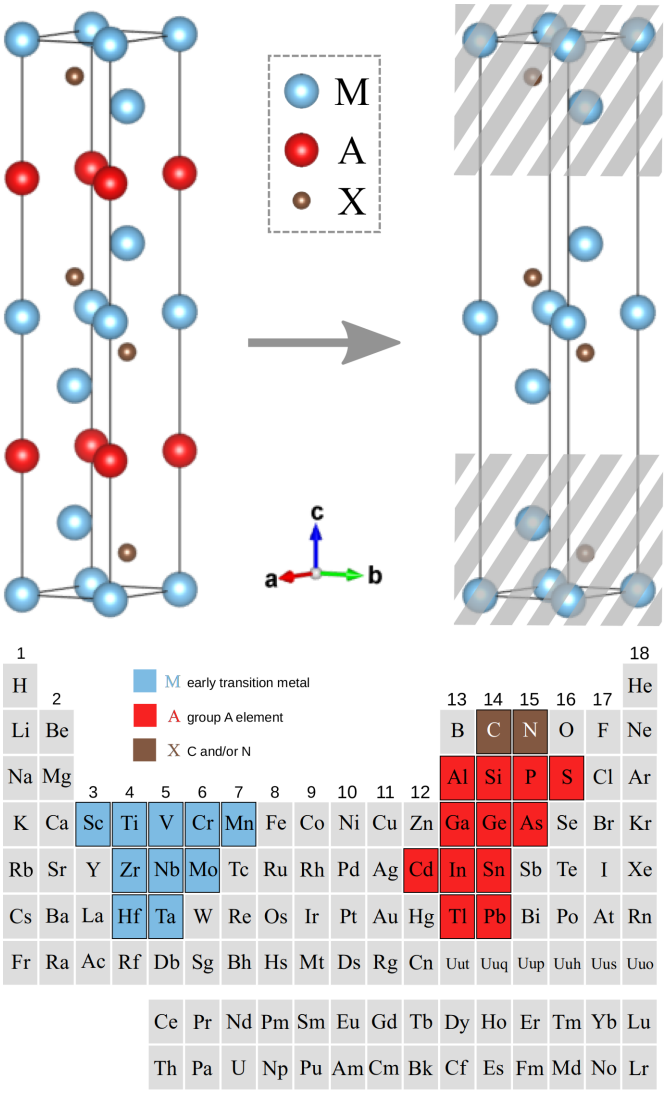

FIG. 1: The primitive cell of a M_3AC_2 MAX-phase[17] (top-left panel), alongside the primitive cell of the resulted M_3C_2 MXene[17] (top-right panel). The blue spheres represent the M atoms, the red the A atoms, and the brown the C atoms. The bottom panel indicates the location, in the periodic table, of the components of a MAX phase.

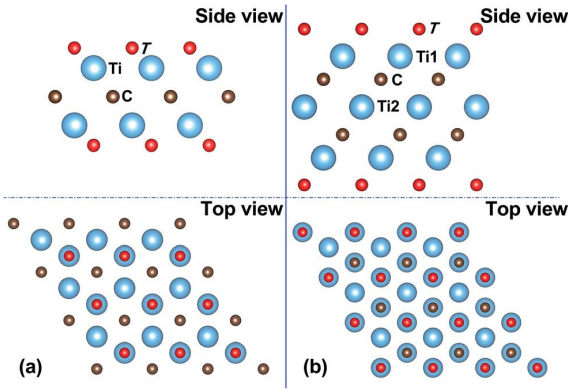

FIG. 2: Side and top views of crystal structures of a 2D MXene monolayer: (a) Ti_2CT_2 and (b) $Ti_3C_2T_2$. Republished with permission of the Royal Society of Chemistry, from Dependence of elastic and optical properties on surface terminated groups in two-dimensional MXene monolayers: a first-principles study, Bai, Y., Zhou, K., Srikanth, N., Pang, J. H., He, X., Wang, R., 6(42), 2016; permission conveyed through Copyright Clearance Center, Inc.

III. MXENE PROPERTIES

A. Mechanical Properties

Depending on the surface terminations, the mechanical properties of an MXene may show significant differences. Bai et al.[16], determined for Ti_2C and Ti_3C_2 that there is a stronger interaction between the O terminations and Ti atoms than in the F or OH terminated MXenes. In addition, the O-terminated MXenes have very high stiffness, and this is attributed to the bonding strength between Ti-O, which is higher than in the Ti-OH and Ti-F cases. Magnuson et al.[19] also found that the surface groups withdraw charge from the Ti-C bonds and weaken them. In particular, they found that the Ti-C bond is longer in Ti_2C-T_x than in Ti_3C_2-T_x, a fact they suggest could affect the elastic properties of the materials. The authors also suggested that the modification of the bond strength can be used to optimize the elasticity. In addition, Zha et al.[20] suggested that O-terminated MXenes should be the first choice for applications regarding structural materials, supercapacitors and so on, due to their larger mechanical strength.

Regarding the strain MXenes can withstand, Chakraborty et al.[21] showed that boron (B) doped Ti_2CO_2, where B substitutes the C atoms, exhibits higher critical strain (by about 100%) compared to the bare MXene. This fact is attributed to a weaker Ti-B bond when compared to the Ti-C bond. Theoretically, Ti_2CO_2-based composites have been found to withstand large strain under uniaxial and biaxial tension[22].

Moreover, Yorulmaz et al.[23], by calculating the Young modulus noted that, for the carbides, the MXene gets stiffer as the mass of the transition metal M increases. This result could not be replicated for the nitrides.

The vast majority of carbide-based MXenes are considered mechanically stable, which is not the case for nitride-based MXenes. In general, single MXene flakes are unstable in environments that contain oxygen and water[24,25]. However, they are relatively stable in water where oxygen has been removed or in dry air.

MXenes in general have lower strength and stiffness than graphene. Despite this fact, molecular dynamics calculations have predicted high enough rigidity for Ti_2C, Ti_3C_2 and Ti_4C_3 MXenes, so that applied surface tension is not enough to overcome it[26–28]. In Fig. 4, we can see the bending rigidity of the $Ti_{n+1}C_n$ MXenes, graphene multilayers, and MoS_2 as a function of their thickness. It is clear that the thicker MXene nanoribbons have higher

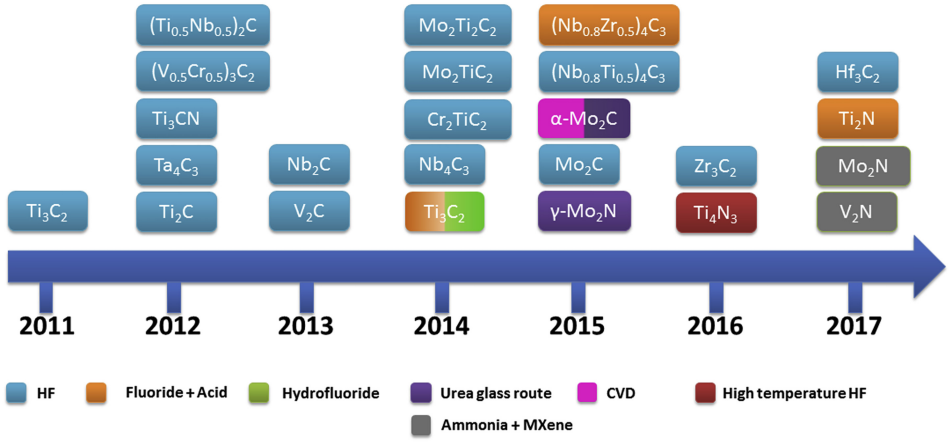

FIG. 3: Timeline of the etching methods used to produce MXenes since the first discovery in 2011, and up to 2017. Reprinted from Chem, 5 (1), Peng, J., Chen, X., Ong, W. J., Zhao, X., Li, N., Surface and heterointerface engineering of 2D MXenes and their nanocomposites: insights into electro and photocatalysis, 18-50, Copyright (2019), with permission from Elsevier.

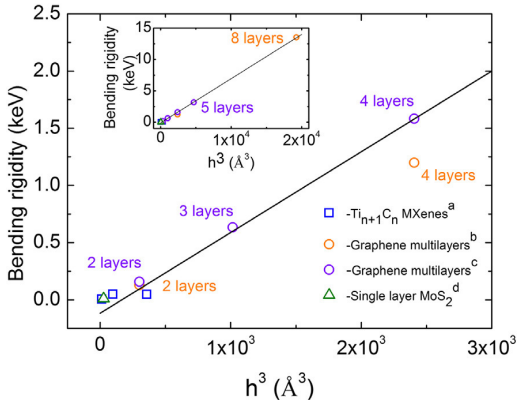

FIG. 4: The bending rigidity of the $Ti_{n+1}C_n$ MXenes, graphene multilayers, and MoS_2 as a function of their thickness h, cubed. Reprinted from Computational Materials Science, 143, Borysiuk, V. N., Mochalin, V. N., Gogotsi, Y., Bending rigidity of two dimensional titanium carbide (MXene) nanoribbons: A molecular dynamics study, 418-424, Copyright (2018), with permission from Elsevier.

values of bending rigidity. The exact value depends on a variety of reasons, such as temperature, and size and shape of the samples.

Finally, surface-modified MXenes were also studied early on in 2013 by Enyashin et al.[29], in particular MXenes terminated with methoxy OCH_3 groups. Their stability was examined by estimating their formation energies ΔH, where it was indicated that a negative value of ΔH is energetically favourable in order to have more stable products. In addition, by calculating the relative total energies, ΔE_{tot}, of $Ti_2C(OCH_3)_2$ and $Ti_3C_2(OCH_3)_2$, it was found that if the methoxy groups are placed above the hollow sites between the three neighbouring carbon atoms within the MXene layer (see Fig. 1), the structure is more stable than when placing the methoxy group above a Ti atom.

The great potential of MXenes for applications in structural composites[30] remains to be explored, provided that bulk quantities can be produced.

B. Electronic Properties

Perhaps the most important electronic property of MXenes is their high electronic conductivity. Most bare MXenes and the majority of those with surface terminations exhibit a metallic behaviour. In recent years, an attempt is being made to increase the MXene metallic conductivity, although the first discovered $Ti_3C_2T_x$, which is also the most studied one[31], is still the most conductive.

The focus has been on developing new $M_{n+1}X_n$ chemistries that will result in higher conductivity by controlling the surface terminations. However, the studies made in that regard lack experimental validation[32]. A different approach to affect MXene conductivity is cation or organic-molecule intercalation where, for stacked materials, the resistance of the device can be increased by over an order of magnitude[32,33]. Figure 5 shows the temperature dependent electrical conductivity of various Mo-based MXenes where there is a rapid increase above 500K.

Zhang et al.[34] in 2018 showed that OH-terminated MXenes exhibit nearly free electron states, located outside the surface atoms and parallel to the surface. These states concentrate in regions where the positive charge is the highest and provide almost perfect transmission channels for electron transport. Moreover, during their experiments, O-terminated MXenes, for example $Ti_{n+1}C_nO_2$, exhibited lower electrical conductivity than the ones terminated with F and OH, that is, $Ti_{n+1}C_nF_2$ and $Ti_{n+1}C_n(OH)_2$ respectively.

Despite the fact that the simulated non-terminated MXenes are all metallic, upon surface functionalization

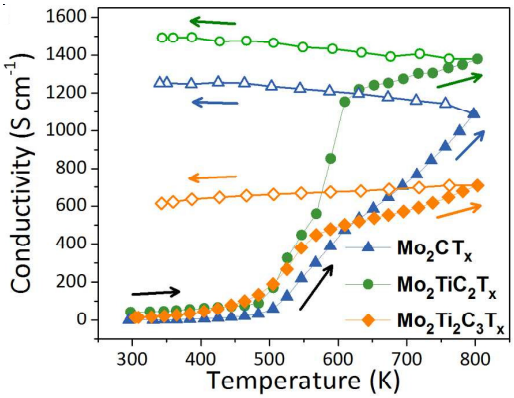

FIG. 5: The temperature dependent electrical conductivity of various Mo-based MXenes. The increase in conductivity results to a decrease in resistivity.

Reprinted (adapted) with permission from Kim, H., Anasori, B., Gogotsi, Y., Alshareef, H. N. (2017). Thermoelectric properties of two-dimensional molybdenum-based MXenes. Chemistry of Materials, 29(15), 6472-6479. Copyright (2017) American Chemical Society.

some of them become semiconducting[35] with a band gap as large as 0.194eV (W_2CO_2). Due to electron transfer from the transition metal to the electronegative surface terminations, the transition metal exhibits lower density of states (DOS) at Fermi level[36,37]. At the moment, no MXene semiconductors have been experimentally realized, although many are theoretically predicted taking under consideration a wide band gap for all surface terminations[37].

In addition, there have been cases where simulated MXenes were predicted to be topological insulators[38,39]. In this category of materials, redtheir edge states are conducting but they exhibit insulating properties on the surface[40]. Currently, in all of the studies on topological behaviour of MXenes, only O- or F-terminated ones have been taken under consideration. None of the insulator MXenes though have been observed experimentally, considering the fact that only ones with mixed terminations have been practically obtained. Control of the surface terminations is once again the key for obtaining this kind of materials.

In general, processes like doping[41], strain application[42], stacking[43], and alloying[44] can control a material's electronic structure. MXenes can withstand a lot of strain (see Subsection III A), so strain engineering has attracted considerable attention[45]. For example, Yu et al.[46] found an indirect-to-direct band gap transition in Ti_2CO_2, Zr_2CO_2, and Hf_2CO_2 when applying biaxial strains 4%, 10%, and 14%, respectively.

Most of the studies regarding the electrical properties of the Ti_3C_2 MXene, have focused on modifying the surface terminations via thermal treatment[47,48]. However, it was determined[49] that when calcination temperature is increased to 800 °C, the Ti_3C_2 nanosheets collapse and the 2D nanostructure is destroyed.

An additional method to manipulate the electrical properties of an MXene is by using reinforcing materials. An example is chitosan[50], a kind of fibre obtained from the exoskeleton of shellfish and insects, where the reinforced MXene exhibits gradient increase of its electrical resistivity as the amount of chitosan increases incrementally.

C. Magnetic Properties

Materials with strong and controllable magnetic moments are important to applications of spintronic devices. Despite the variety of MXenes, the ground states of the majority of them, bare or otherwise, are non-magnetic. This is attributed to the strong covalent bond between the transition metal and the X element[35]. Some bare MXenes though have been predicted to be intrinsically magnetic. These include Cr_2C[51] and Ti_2N[52] (ferromagnetic), and Cr_2N[53] and Mn_2C[54] (anti-ferromagnetic). The magnetism in the case of MXenes can be[55]:
a) intrinsic properties of the transition metal
b) defects in monolayers
c) surface terminations.

As stated before, the most common MXenes, including Ti_3C_2, are non-magnetic, however there are cases where different magnetic structures were reported. For example, Dong et al.[56] determined that $Ti_2MnC_2T_x$ MXenes are ferromagnetic in the ground states, regardless of the nature of the surface terminations. $Ti_2MnC_2T_x$ belongs to a new family of ordered double-transition-metal MXenes[57,58] which have one or two layers of a transition metal sandwiched between the layers of another one. In 2018, Sun et al.[59] studied double-transition-metal MXenes with Ti atoms as the central layer and showed that different terminations and cation configurations lead to a variety of magnetic orders and properties different from the single transition metal carbides known thus far.

In 2017, reports about a novel MAX phase with in-plane chemical order were made[60,61]. These compounds were called i-MAX and have the general formula $(M_{2/3}M'_{1/3})_2AX$. From i-MAX phases, came the i-MXenes after etching the A-element atoms (e.g. $W_{4/3}C$ and $Nb_{4/3}C$[62,63]). Prior to that, Zhu et al.[64] had found for Nb_2C a theoretical in-plane lattice constant value in agreement with the experimental one, and showed that the energetically favorable site for Li adsorption is located on top of C. In 2020, Gao et al.[65], turned their attention to the magnetic properties of i-MXenes with a general formula $(M_{2/3}M'_{1/3})_2X$. In particular, by performing density functional theory (DFT) calculations, they examined the cases where M', i.e. the dopant element, is magnetic and one of the transition metals except Tc. Out of 319 i-MXenes, they found 62 cases that they were magnetic. In addition, 6 can change their magnetic configuration, depending on their geometries (rectangular or hexagonal) which in turn need a strain to be applied. Therefore, the magneto-crystalline anisotropy of

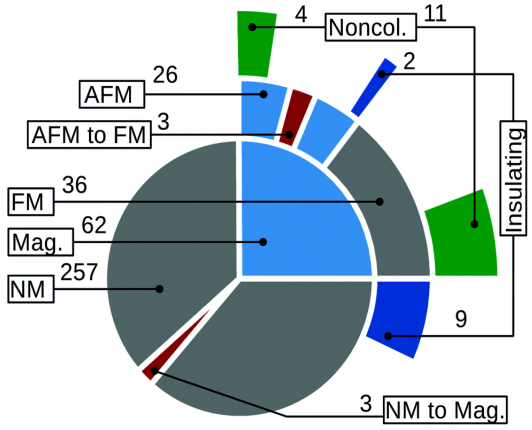

FIG. 6: Classification of the magnetic ground states for the 319 i-MXenes. Mag=Magnetic, NM=Non-Magnetic, AFM=Antiferromagnetic, FM=Ferromagnetic, Noncol=Noncollinear Magnetic Structure. 'NM-to-Mag' and 'AFM to FM' mark the compounds whose ground state changes by imposing hexagonal geometry. Republished with permission of Royal Society of Chemistry, from Magnetic i-MXenes: a new class of multifunctional two-dimensional materials, Gao, Q., Zhang, H., 12(10), 2020; permission conveyed through Copyright Clearance Center, Inc.

i-MXenes can be enhanced.

In Figure 6, we can see the classification of the magnetic ground states for the 319 i-MXenes.

An extensive theoretical study of the magnetic properties of nitrogen-based MXenes, which have an extra electron per unit cell when compared to carbon-based ones, was carried out by Kumar et al[66]. The authors suggested a simple model to predict the magnetic behaviour of M_2NT_2 based on the assumption that only electrons occupying the non-bonding d-orbitals can contribute to magnetism. By applying their model to M_2NT_2 MXenes with transition metals belonging to the third period of the periodic table, they identified five nitride MXenes (Mn_2NF_2, Mn_2NO_2, $Mn_2N(OH)_2$, Ti_2NO_2, and Cr_2NO_2) with robust ferromagnetic ground states. Curie temperatures for all terminations were also well above the room temperature, a fact that made the magnetically ordered phases stable.

In 2018, Bandyopadhyay et al.[67] investigated the point defect formation mechanisms in MXenes. They found that few of the defective MXenes acquire a magnetic nature because of unpaired electrons in the spin split d-orbitals. Therefore, they suggested that intrinsic point defects can be used to modify the magnetic properties of MXenes.

Moreover, Scheibe et al.[55] in 2019, investigated the influence the different terminations have on the magnetic properties of $Ti_3C_2T_x$. They found that the bare TiC samples exhibit paramagnetic behavior, similarly to the samples with F or S-based terminations, but if the sample contained two kinds of terminations, then its behaviour was shifted to ferromagnetic/paramagnetic. Therefore, the magnetic properties of $Ti_3C_2T_x$ can be altered via modulation of the surface terminations. Another example of the impact of the terminations is described in Ref. [68]. When Cr_2C is terminated by F, H, OH or Cl groups, it will be transformed from a ferromagnetic half metal into an antiferromagnetic semiconductor.

The potential use of MXenes in spintronics makes the methods to control their magnetism a rapidly advancing field.

D. Optical Properties

Regarding optics, various interesting features of MXenes have been demonstrated in the past few years. These include optical transparency, plasmonic behavior, and efficient photothermal conversion. The ability of MXenes to interact with light in multiple ways has had a significant impact on the research community[69]. Once again, it is the surface terminations that play the most significant part in determining a material's optical properties.

Berdiyorov[70] in 2016 investigated the role of surface terminations on the optical properties of $Ti_3C_2T_2$ (T=F, O, OH) MXenes and compared the results to the bare MXene Ti_3C_2. Using the dielectric constant, Berdiyorov calculated the refractive index, n, and the extinction coefficient, k, for all samples and found that at low photon energies, E, the terminations reduced n, while at higher E ($>$ 1eV), n was enhanced. The surface terminations also resulted in the reduction of k for most of the photon energy range. In addition, at even larger photon energies ($E >$ 5eV) the terminations resulted in stronger absorption as compared to the bare MXene. Finally, in the ultraviolet region of the spectrum (5eV $< E <$ 10eV), all surface terminations resulted in larger reflectivity as compared to the bare MXene.

Halim et al.[71] by studying Ti_2CT_x and Nb_2CT_x films, showed a different approach to control the optical properties of MXenes is to change the nature of the transition metal. They found that the Nb-based films showed an increase in absorption towards the infrared spectral range. This behaviour significantly differed from that of the corresponding MAX phase Nb_2AlC, a fact that was not observed for the Ti-based films. Halim et al.[71] suggested that the difference in the optical properties lay within the electronic configuration of the transition metals (Ti is in group 4 and Nb is in group 5 of the periodic table) and their bonding with the C atoms and surface terminations.

In 2017, Li et al.[72] showed that MXenes exhibit higher capability to absorb light than carbon nanotubes (CNT). In addition, Jiang et al.[73] in 2018, examined the optical non-linearity of $Ti_3C_2T_x$ using excitation sources with various wavelengths (800nm, 1064nm, 1550nm and 1800nm). They found absorption response two orders of magnitude larger than other processes but the refractive index was comparable to that of graphene. Finally, for Ti_2C, Ti_2N, Ti_3C_2, and Ti_3N_2, for $E <$ 1eV, the reflec-

tivity has been found to reach 100%, which means that these materials have the ability to transmit electromagnetic waves[74].

In general, it is believed that both the linear (e.g. absorption) and nonlinear (e.g. refractive index) optical properties of MXenes are highly dependent on the energy structures (e.g. energy bandgap, direct/indirect bandgap, topological insulators, etc.)[74].

IV. APPLICATIONS

Since they were first discovered in 2011, MXenes have received significant attention. Studies have revealed their potential applications in energy storage, optoelectronics, spintronics and catalysis, and even in environmental and biological issues. Below we summarize the most recent applications, with a particular focus on energy storage.

A. Energy Storage and Conversion

Energy storage and conversion has been a key scientific challenge for years, since the materials used for these applications need to be light, flexible, conductive, and have large surface-to-mass ratio [specific surface area (SSA)(m^2g^{-1})][75]. Carbon black has $SSA < 900m^2g^{-1}$[76] while carbon nanotubes (CNT) have $SSA = 100 - 1000m^2g^{-1}$[77]. A sheet of graphene, on the other hand, has theoretically very large surface-to mass ratio, $SSA = 2630m^2g^{-1}$[77], a value that is similar to that of the activated carbon[78]. Other 2D materials that can be used for energy storage are the transition metal dichalcogenides (TMD) like WS_2, in combination with graphene[79].

MXenes are a new class of 2D crystals that can be used in energy applications. Compared to materials like graphene, MXenes have much smaller specific surface area. For example, experimentally produced $Ti_3C_2T_x$ has SSA up to $66m^2g^{-1}$ and V_2CT_x up to $19m^2g^{-1}$[80], while theoretically $Ti_3C_2T_x$ can reach up to $496m^2g^{-1}$. Ren et al.[81] in 2016, managed to produce porous $Ti_3C_2T_x$ MXenes (p-MXenes) using a transition metal salt and acid treatment. They determined that the p-$Ti_3C_2T_x$ MXene had SSA increased from 19.6 (pristine $Ti_3C_2T_x$) to $93.6m^2g^{-1}$. Furthermore, a high specific capacity of $\approx 1250mAhg^{-1}$ was revealed for p-$Ti_3C_2T_x$/CNT electrodes. Graphene electrodes on the other hand, when chemically modified, can reach $\approx 1200mAhg^{-1}$[82] while Hassoun et al.[83] in 2014 showed that electrodes based on Cu-supported graphene nanoflakes ink can reach specific capacities of $\approx 1500mAhg^{-1}$. Both these values are close or even larger than the corresponding ones for the MXenes.

Regarding volumetric capacity, functionalized graphene shows results up to $200Fg^{-1}$[78,84,85], while for MXenes, researchers were able to achieve for Ti_3C_2 $320Fg^{-1}$ as early as in 2014[86].

At present, Li-ion batteries do not operate satisfactorily in large-scale operations like sustaining a clean power grid[87]. Intercalation pseudocapacitance[88], which occurs through bulk redox reactions with ultrafast ion diffusion[89,90], has risen as an alternative chemistry for advanced electrochemical energy storage devices. The intercalation pseudocapacitors have many benefits, considering the limited exposure of the surface to the electrolyte. This leads to a decrease of the irreversible surface reactions due to electrolyte decomposition, without affecting the charge storage[91]. MXenes pose as good materials for these pseudocapacitors as their morphology minimizes the surface which interacts with the electrolytes, and their really small interlayer spacing makes for fast ion intercalation.

In 2012, shortly after their discovery, Naguib et al.[92] studied the MXene's Ti_2C use as anode for lithium-ion batteries. They found that Ti_2C had reversible capacity five times higher than the corresponding MAX phase Ti_2AlC, exhibiting a stable capacity of $225mAhg^{-1}$. They suggested that the results were promising for the use of MXenes as Li^+ intercalation electrodes in lithium-ion batteries[92]. Since then, other batteries have been examined, for example sodium-ion, pottasium-ion and lithium-sulfur[93–95].

In 2015, Zhu et al.[64], investigated the Li adsorption in monolayer Nb_2C and Nb_2CX_2 MXenes and found that the most energetically favourable site for Li adsorption was on top of the C atom. They also showed that, since Li forms clusters on $Nb_2C(OH)_2$ and LiF forms clusters on Nb_2CF_2 and $Nb_2CO_{1,5}F_{0,5}$, OH and F terminations must be avoided in battery applications. Moreover, Nb_2C was found the most promising electrode material for Li-ion batteries because of its low diffusion barrier.

In addition, Zhu et al. in 2016[96] replaced OH, F, and O terminations with S and predicted high electric conductivities and cycling rates for Li-ion batteries using Zr-based MXenes. The lifetime of the battery was also found not affected by by-products like dendrites.

More recently, in 2019, Shukla et al.[97] studied S-terminated MXenes (V_2NS_2 and Ti_2NS_2) as anodes for Li/Na ion batteries. They found that multilayer ion intercalation is possible, and that the materials manifest high capacity, especially for the Li case. Regarding ionic diffusion, the authors showed that the lower energy barriers result in ultra fast diffusion. Furthemore, at the same year, Zhang et al.[98] showed that MXenes can be used as a conductive binder for Si electrodes in order to decrease the inactive volume of the electrode and have better battery performance. Moreover, the $Ti_3C_2T_x$ MXene was found useful as a reinforcing material for polymers such as polyvinyl alcohol (PVA), where the strong films fabricated can be used as electrodes for supercapacitors[99,100].

In addition, Wang et al.[101] studied Ti_3C_2 MXenes as the S cathode host for LiS batteries. They showed that the bare MXene cannot be used directly for this purpose due to decomposition. However, S and O terminated Ti_3C_2 can achieve high performance.

In 2020, Li et al.[102] investigated the use of chalcogenated Ti_3C_2 as an anode material for Li-ion batteries. Chalcogenation gave the $Ti_3C_2T_2$, $T = O$, S, Se and Te, MXene enhanced Li-ion accessibility and mobility while $Ti_3C_2S_2$ and $Ti_3C_2Se_2$ MXene electrodes yielded a theoretical Li-storage capacity of $462.61 mAhg^{-1}$ and $329.32 mAhg^{-1}$ respectively. The authors noted that the fabrication of MXenes with larger interlayer spacing could achieve higher Li-storage capacity.

To summarize, if we were to compare graphene with MXenes as materials for anodes for Li-ion batteries, despite the fact that graphene has larger SSA and higher capacity, we should also take into consideration that graphene electrodes do not allow fast enough diffusion for energy applications that require high power output[103]. Furthermore, graphene's low lithiation potential enables the formation of lithium dendrites which are flammable and limit the cycling stability of the battery cells[104,105]. In contrast, MXenes have higher lithiation potential and wider interlayer spacing[1,106], which allows for fast ion intercalation. Add to that fact graphene's limited commercial use, mainly due to its expensiveness, MXenes seem currently the most promising materials for battery applications.

B. Other Applications

Apart from energy storage devices, Sarycheva et al.[107] reported the use of MXenes for antenna applications. In particular, they constructed the first radio-frequency (RF) MXene devices for wireless communication and showed that MXene antennas need lower thickness in order to work than those of the best-known metals, enabling ultra-thin and transparent wireless devices.

Blanco et al.[108] determined that MXene nano-sheets showed unique catalytic properties for the hydrodeoxygenation (i.e., a process to remove oxygen) of guaiacol in order to make it more stable. In addition, in Ref. [109], MXenes were studied as energy-efficient alternatives to the Haber-Bosch process which is used in the production of ammonia. To this end, Mo_2TiC_2 was examined as an electrocatalyst and the authors proved through the analysis of Gibbs free energy, that it could be a new, effective material for ammonia synthesis.

Apart from the aforementioned environmetnal uses, MXenes have also been used for the removal of heavy metals from water. For example, Shahzad et al.[110] developed a system to remove copper from water using $Ti_3C_2T_x$ MXenes. XRD analysis showed that copper reacts strongly with the surface terminations of the MXenes, resulting in surface oxidation.

MXenes have also been found useful in biological applications. Szuplewska et al.[111] examined the biocompatibility of Ti_2NT_x towards human skin malignant melanoma cells and human breast cancer cells. They determined that the multi-layered Ti_2NT_x shows higher toxicity towards cancerous cells when compared to normal ones, thus revealing the potential use of MXenes in biotechnology and nanomedicine. Moreover, MXenes have been used in various bioimaging techniques[112] such as fluorescence microscopy, where MXene's fluorescence properties are enhanced by attaching a fluorescence species to their surface[113], *in vitro* bioimaging using quantum dots[114,115], and X-Ray computed tomography (CT) where MXenes are used as imaging contrast elements[116–118].

The properties of MXenes also make them suitable materials for sensors. For instance, Liu et al.[119] proposed a nitrite bio-sensor containing hemoglobin (Hb) immobilized on Ti_3C_2 which was used to detect the presence of nitrite in water samples. They proposed Ti_3C_2 MXenes as suitable candidates for enzyme immobilization, as they can provide a safe micro-environment for the proteins. In addition, Rakhi et al.[120] developed a glucose bio-sensor based on an Au/MXene nanocomposite to detect glucose in the presence of other electroactive substances. Crystalline Au nanoparticles where placed on the surface of $Ti_3C_2T_x$ Mxenes and an improved electrical conductivity was found, making the Au/MXene composite a good enzyme immobilization matrix. Another study in 2017 by Muckley at al.[121], proposed the used of MXenes as sensors for water and humidity in air, while Ma et al.[122] in the same year constructed MXene-based sensors to detect human activities such as swallowing, coughing, jointbending.

In 2019, Montazeri et al.[123] devised MXene/GaAs/MXene photodetectors and showed that they have higher responsivity, quantum efficiency and dynamic range than the current Ti/AuGaAsTi/Au devices, proving MXenes also useful in the optoelectronics and microelectronics industries.

Finally, MXenes' structure allows for distance between atomic layers and changes in conductivity when external pressure is applied[124]. Tan et al.[124] used MXene-based pressure sensors and, by designing an optoelectronic spiking afferent nerve, they were able to detect Morse code, braille, object movement, and handwritten words, showing promise for human-machine interaction technologies.

In Figure 7 we can see summarized the applications of MXenes beyond energy storage, as presented in this paper.

V. SUMMARY AND FUTURE DIRECTIONS

In the present paper, we provided an overview of the methods for the synthesis of MXenes from the corresponding MAX phases, alongside the advantages and disadvantages of each method. In addition, we described the mechanical, electronic, magnetic, and optical properties of MXenes. The ability to manipulate the MXenes' terminations, led to materials with large mechanical strength, high conductivity, intrinsic magnetism, strong absorption and large reflectivity. In addition, we outlined the most recent applications of MXenes, focusing

Application	Description	References
Antennas	RF MXene devices for wireless communication	107
Catalysts	hydrodeoxygenation of guaiacol, electrocatalyst for ammonia synthesis	108 - 109
Water purification	copper removal from water	110
Anti-cancer	toxicity towards cancerous cells	111
Bioimaging	fluorescence microscopy, quantum dots, CT scans	112 , 114 - 118
Sensors	presence of nitrite in water samples, glucose bio-sensor, water and humidity in air, human activities such as swallowing, coughing, joint bending etc	119 - 122
Photodetectors	MXene/GaAs/Mxene photodetectors with high responsivity, quantum efficiency and dynamic range	123
Pressure sensors	human-machine interaction	124

FIG. 7: Summary of the most recent applications of MXenes beyond energy storage, as referenced in this paper.

on energy storage, which are summarized in Fig. 7.

The latest results show that MXenes composed of transition metal elements of group 6 of the periodic system (Cr, Mo, W), are the most promising ones for superconductivity, at least in the case of Mo and W[125]. In addition, Luo et al.[126] in 2020 have, for the first time, examined the tensile behavior of $Ti_3C_2T_x$. They found that the number of defects influences significantly the overall mechanical properties of the films, a fact that is reflected by the dependency of their tensile strength, elastic modulus and fracture strain on thickness.

Numerous scientific reports are published yearly regarding the MXenes' possible applications. However, there are several gaps in the current knowledge that need to be addressed.

Despite the amount of theoretical studies regarding their use in energy storage devices, the charge storage mechanism of the MXenes is not fully understood yet, neither are the effects of their different compositions on their performance as electrodes. Moreover, MXenes' stability and durability are still important challenges. MXene nanosheets degrade quickly when in contact with water and oxygen, making their use in various applications difficult[127].

Another significant problem is the fact that, for many MXenes studied through computational techniques, there is no precursory MAX-phase[25], for example W_2C. The attention should be turned into the synthesis of new layered materials that could be used for the production of MXenes. In that respect, a way to access more MXene compositions is by the synthesis of quaternary MAX phases. Quaternary MAX phases lead to the formation of MAX phases with elements (for example bismuth) that are not present in the synthesis of ternary MAX phases[128–131]. In addition, the terminations and their different characterizations after synthesis need to be examined, alongside the methods for achieving uniform terminations. Bare MXenes have not yet been produced, despite being predicted as metallic conductors. Moreover, the studies of the interaction of the MXenes with light are at a very early stage[73]. The non-linear optical phenomena regarding MXenes are still unexplored for the materials to be widely used in photonic applications. Studies on the toxicity of MXenes are also limited.

Currently there are more than 30 MXene composites, and more are being discovered daily. MXenes have demonstrated potential as next-generation materials in various fields, although they are mainly produced at laboratories and have small yield. If large-scale production was to be achieved, then MXenes would have a larger impact on a commercial scale. Dozens more MXene structures have been examined at a theoretical level using computational methods, contributing to the rapid advances in the field.

When it comes to environmental applications, many MXenes and MXene-based composites have been proposed for processes like water purification, desalination, etc[132]. Furthermore, the removal of pollutants from the environment is still a challenge which could be resolved by further studies on the MXenes[133].

Biomedicine is another field that has shown it can be benefited from the use of MXenes, with studies on cancer treatment, bio-sensors, neural electrodes, dialysis and theranostics[87,134] being a research topic that has significantly expanded during the past two years[135].

MXenes have also started taking over from other nanomaterials like graphene in electromagnetic applications, for example RF antennas[107] and electromagnetic interference (EMI) shielding.

The production, storage and utilization of fuels to combat the ever-increasing energy consumption globally is also an issue that can be addressed via MXenes, due to their physical and chemical properties. Currently, Li-ion batteries are the largest power source in both small portable electronics, and electric vehicles[133]. However, with problems such as safety, limited natural lithium resources and production cost[136,137], there is a need for the development of non-lithium batteries.

Perhaps the biggest challenge yet, though, is the experimental validation of all the theoretical studies, and the verification of the predicted properties of MXenes.

Acknowledgments

The authors acknowledge support from the International Consortium of Nanotechnologies (ICON) funded by Lloyds Register Foundation, a charitable foundation which helps to protect life and property by supporting engineering-related education, public engagement and the application of research.

Data Availability

Data sharing is not applicable to this article as no new data were created or analyzed in this study.

* Electronic address: ac0966@coventry.ac.uk

[1] M. Naguib, M. Kurtoglu, V. Presser, J. Lu, J. Niu, M. Heon, L. Hultman, Y. Gogotsi, and M. W. Barsoum, Advanced Materials **23**, 4248 (2011).

[2] L. Verger, V. Natu, M. Carey, and M. W. Barsoum, Trends in Chemistry (2019).

[3] M. W. Barsoum and T. El-Raghy, American Scientist **89**, 334 (2001).

[4] Z. Sun, International Materials Reviews **56**, 143 (2011).

[5] M. Radovic and M. W. Barsoum, American Ceramics Society Bulletin **92**, 20 (2013).

[6] X. Li, Z. Huang, and C. Zhi, Front. Mater. 6: 312 (2019).

[7] J. Zhou, X. Zha, X. Zhou, F. Chen, G. Gao, S. Wang, C. Shen, T. Chen, C. Zhi, and P. Eklund, ACS nano **11**, 3841 (2017).

[8] M. H. Tran, T. Schafer, A. Shahraei, M. Durrschnabel, L. Molina-Luna, U. I. Kramm, and C. S. Birkel, ACS Applied Energy Materials **1**, 3908 (2018).

[9] M. Ghidiu, M. R. Lukatskaya, M.-Q. Zhao, Y. Gogotsi, and M. W. Barsoum, Nature **516**, 78 (2014).

[10] L. Ma, L. R. L. Ting, V. Molinari, C. Giordano, and B. S. Yeo, Journal of Materials Chemistry A **3**, 8361 (2015).

[11] C. Xu, L. Wang, Z. Liu, L. Chen, J. Guo, N. Kang, X. L. Ma, H. M. Cheng, and W. Ren, Nature Materials **14**, 1135 (2015).

[12] P. Urbankowski, B. Anasori, T. Makaryan, D. Er, S. Kota, P. L. Walsh, M. Zhao, V. B. Shenoy, M. W. Barsoum, and Y. Gogotsi, Nanoscale **8**, 11385 (2016).

[13] T. Li, L. Yao, Q. Liu, J. Gu, R. Luo, J. Li, X. Yan, W. Wang, P. Liu, and B. Chen, Angewandte Chemie International Edition **57**, 6115 (2018).

[14] S. Yang, P. Zhang, F. Wang, A. G. Ricciardulli, M. R. Lohe, P. W. Blom, and X. Feng, Angewandte Chemie **130**, 15717 (2018).

[15] W. Sun, S. Shah, Y. Chen, Z. Tan, H. Gao, T. Habib, M. Radovic, and M. Green, Journal of Materials Chemistry A **5**, 21663 (2017).

[16] Y. Bai, K. Zhou, N. Srikanth, J. H. Pang, X. He, and R. Wang, RSC Advances **6**, 35731 (2016).

[17] A. Jain, S. P. Ong, G. Hautier, W. Chen, W. D. Richards, S. Dacek, S. Cholia, D. Gunter, D. Skinner, and G. Ceder, APL Materials **1**, 011002 (2013).

[18] J. Peng, X. Chen, W.-J. Ong, X. Zhao, and N. Li, Chem **5**, 18 (2019).

[19] M. Magnuson, J. Halim, and L.-Å. Näslund, Journal of Electron Spectroscopy and Related Phenomena **224**, 27 (2018).

[20] X.-H. Zha, K. Luo, Q. Li, Q. Huang, J. He, X. Wen, and S. Du, EPL (Europhysics Letters) **111**, 26007 (2015).

[21] P. Chakraborty, T. Das, D. Nafday, L. Boeri, and T. Saha-Dasgupta, Physical Review B **95**, 184106 (2017).

[22] A. Muzaffar, M. B. Ahamed, and K. Deshmukh, Materials Research Foundations **51**, 105 (2019).

[23] U. Yorulmaz, A. Özden, N. K. Perkgöz, F. Ay, and C. Sevik, Nanotechnology **27**, 335702 (2016).

[24] O. Mashtalir, K. M. Cook, V. N. Mochalin, M. Crowe, M. W. Barsoum, and Y. Gogotsi, Journal of Materials Chemistry A **2**, 14334 (2014).

[25] B. Anasori, M. R. Lukatskaya, and Y. Gogotsi, Nature Reviews Materials **2**, 1 (2017).

[26] S. Prolongo, R. Moriche, A. Jiménez-Suárez, M. Sánchez, and A. Ureña, European Polymer Journal **61**, 206 (2014).

[27] V. N. Borysiuk, V. N. Mochalin, and Y. Gogotsi, Nanotechnology **26**, 265705 (2015).

[28] V. N. Borysiuk, V. N. Mochalin, and Y. Gogotsi, Computational Materials Science **143**, 418 (2018).

[29] A. N. Enyashin and A. L. Ivanovskii, The Journal of Physical Chemistry C **117**, 13637 (2013).

[30] A. Lipatov, H. Lu, M. Alhabeb, B. Anasori, A. Gruverman, Y. Gogotsi, and A. Sinitskii, Science Advances **4**, eaat0491 (2018).

[31] C. J. Zhang, S. Pinilla, N. McEvoy, C. P. Cullen, B. Anasori, E. Long, S. H. Park, A. Seral-Ascaso, A. Shmeliov, D. Krishnan, et al., Chemistry of Materials **29**, 4848 (2017).

[32] J. L. Hart, K. Hantanasirisakul, A. C. Lang, B. Anasori, D. Pinto, Y. Pivak, J. T. van Omme, S. J. May, Y. Gogotsi, and M. L. Taheri, Nature Communications **10**, 1 (2019).

[33] H. Kim, B. Anasori, Y. Gogotsi, and H. N. Alshareef, Chemistry of Materials **29**, 6472 (2017).

[34] N. Zhang, Y. Hong, S. Yazdanparast, and M. A. Zaeem, 2D Materials **5**, 045004 (2018).

[35] M. Khazaei, A. Ranjbar, M. Arai, T. Sasaki, and S. Yunoki, Journal of Materials Chemistry C **5**, 2488 (2017).

[36] A. L. Ivanovskii and A. N. Enyashin, Russian Chemical Reviews **82**, 735 (2013).

[37] K. Hantanasirisakul and Y. Gogotsi, Advanced Materials **30**, 1804779 (2018).

[38] M. Khazaei, A. Ranjbar, M. Arai, and S. Yunoki, Physical Review B **94**, 125152 (2016).

[39] C. Si, K. H. Jin, J. Zhou, Z. Sun, and F. Liu, Nano Letters **16**, 6584 (2016).

[40] H. Weng, A. Ranjbar, Y. Liang, Z. Song, M. , S. Yunoki, M. Arai, Y. Kawazoe, Z. Fang, and X. Dai, Physical Re-

view-B-**92**,-075436-(2015).-
[41] H.-P.-Komsa,-J.-Kotakoski,-S.-Kurasch,-O.-Lehtinen,-U.-Kaiser,-and-A.-V.-Krasheninnikov,-Physical-Review-Letters-**109**,-035503-(2012).-
[42] B.-Amin,-T.-P.-Kaloni,-and-U.-Schwingenschlögl,-RSC-Advances-**4**,-34561-(2014).-
[43] B.-Amin,-N.-Singh,-and-U.-Schwingenschlögl,-Physical-Review-B-**92**,-075439-(2015).-
[44] H.-P.-Komsa-and-A.-V.-Krasheninnikov,-Physical-Review-B-**88**,-085318-(2013).-
[45] Z.-Fu,-N.-Wang,-D.-Legut,-C.-Si,-Q.-Zhang,-S.-Du,-T.-C.-Germann,-J.-S.-Francisco,-and-R.-Zhang,-Chemical-Reviews-**119**,-11980-(2019).-
[46] X.-f.-Yu,-J.-b.-Cheng,-Z.-b.-Liu,-Q.-z.-Li,-W.-z.-Li,-X.-Yang,-and-B.-Xiao,-RSC-Advances-**5**,-30438-(2015).-
[47] K.-Wang,-Y.-Zhou,-W.-Xu,-D.-Huang,-Z.-Wang,-and-M.-Hong,-Ceramics-International-**42**,-8419-(2016).-
[48] J.-Michael,-Z.-Qifeng,-and-W.-Danling,-Nanomaterials-and-Nanotechnology-**9**,-1847980418824470-(2019).-
[49] H.-Wang,-Y.-Wu,-J.-Zhang,-G.-Li,-H.-Huang,-X.-Zhang,-and-Q.-Jiang,-Materials-Letters-**160**,-537-(2015).-
[50] C.-Hu,-F.-Shen,-D.-Zhu,-H.-Zhang,-J.-Xue,-and-X.-Han,-Frontiers-in-Energy-Research-**4**,-41-(2017).-
[51] C.-Si,-J.-Zhou,-and-Z.-Sun,-ACS-Applied-Materials-&-Interfaces-**7**,-17510-(2015).-
[52] G.-Gao,-G.-Ding,-J.-Li,-K.-Yao,-M.-Wu,-and-M.-Qian,-Nanoscale-**8**,-8986-(2016).-
[53] G.-Wang,-The-Journal-of-Physical-Chemistry-C-**120**,-18850-(2016).-
[54] L.-Hu,-X.-Wu,-and-J.-Yang,-Nanoscale-**8**,-12939-(2016).-
[55] B.-Scheibe,-K.-Tadyszak,-M.-Jarek,-N.-Michalak,-M.-Kempiński,-M.-Lewandowski,-B.-Peplińska,-and-K.-Chybczyńska,-Applied-Surface-Science-**479**,-216-(2019).-
[56] L.-Dong,-H.-Kumar,-B.-Anasori,-Y.-Gogotsi,-and-V.-B.-Shenoy,-The-Journal-of-Physical-Chemistry-Letters-**8**,-422-(2017).-
[57] B.-Anasori,-Y.-Xie,-M.-Beidaghi,-J.-Lu,-B.-C.-Hosler,-L.-Hultman,-P.-R.-Kent,-Y.-Gogotsi,-and-M.-W.-Barsoum,-ACS-Nano-**9**,-9507-(2015).-
[58] B.-Anasori,-C.-Shi,-E.-J.-Moon,-Y.-Xie,-C.-A.-Voigt,-P.-R.-Kent,-S.-J.-May,-S.-J.-Billinge,-M.-W.-Barsoum,-and-Y.-Gogotsi,-Nanoscale-Horizons-**1**,-227-(2016).-
[59] W.-Sun,-Y.-Xie,-and-P.-R.-Kent,-Nanoscale-**10**,-11962-(2018).-
[60] Q.-Tao,-M.-Dahlqvist,-J.-Lu,-S.-Kota,-R.-Meshkian,-J.-Halim,-J.-Palisaitis,-L.-Hultman,-M.-W.-Barsoum,-P.-O.-Persson,-et-al.,-Nature-Communications-**8**,-1-(2017).-
[61] M.-Dahlqvist,-J.-Lu,-R.-Meshkian,-Q.-Tao,-L.-Hultman,-and-J.-Rosen,-Science-Advances-**3**,-e1700642-(2017).-
[62] R.-Meshkian,-M.-Dahlqvist,-J.-Lu,-B.-Wickman,-J.-Halim,-J.-Thörnberg,-Q.-Tao,-S.-Li,-S.-Intikhab,-J.-Snyder,-et-al.,-Advanced-Materials-**30**,-1706409-(2018).-
[63] C.-Zhan,-W.-Sun,-Y.-Xie,-D.-e.-Jiang,-and-P.-R.-Kent,-ACS-Applied-Materials-&-Interfaces-**11**,-24885-(2019).-
[64] J.-Zhu,-A.-Chroneos,-and-U.-Schwingenschlögl,-Physica-Status-Solidi-(RRL)–Rapid-Research-Letters-**9**,-726-(2015).-
[65] Q.-Gao-and-H.-Zhang,-Nanoscale-**12**,-5995-(2020).-
[66] H.-Kumar,-N.-C.-Frey,-L.-Dong,-B.-Anasori,-Y.-Gogotsi,-and-V.-B.-Shenoy,-ACS-Nano-**11**,-7648-(2017).-
[67] A.-Bandyopadhyay,-D.-Ghosh,-and-S.-K.-Pati,-Physical-Chemistry-Chemical-Physics-**20**,-4012-(2018).-
[68] D.-Xiong,-X.-Li,-Z.-Bai,-and-S.-Lu,-Small-**14**,-1703419-(2018).-
[69] K.-Chaudhuri,-Z.-Wang,-M.-Alhabeb,-K.-Maleski,-Y.-Gogotsi,-V.-Shalaev,-and-A.-Boltasseva,-in-*2D Metal Carbides and Nitrides (MXenes)* (Springer,-2019),-pp.-327–346.-
[70] G.-Berdiyorov,-AIP-Advances-**6**,-055105-(2016).-
[71] J.-Halim,-I.-Persson,-E.-J.-Moon,-P.-Kühne,-V.-Darakchieva,-P.-O.-Å.-Persson,-P.-Eklund,-J.-Rosen,-and-M.-W.-Barsoum,-Journal-of-Physics:-Condensed-Matter-**31**,-165301-(2019).-
[72] R.-Li,-L.-Zhang,-L.-Shi,-and-P.-Wang,-ACS-Nano-**11**,-3752-(2017).-
[73] X.-Jiang,-S.-Liu,-W.-Liang,-S.-Luo,-Z.-He,-Y.-Ge,-H.-Wang,-R.-Cao,-F.-Zhang,-Q.-Wen,-et-al.,-Laser-&-Photonics-Reviews-**12**,-1700229-(2018).-
[74] X.-Jiang,-A.-V.-Kuklin,-A.-Baev,-Y.-Ge,-H.-Ågren,-H.-Zhang,-and-P.-N.-Prasad,-Physics-Reports-(2020).-
[75] F.-Bonaccorso,-L.-Colombo,-G.-Yu,-M.-Stoller,-V.-Tozzini,-A.-C.-Ferrari,-R.-S.-Ruoff,-and-V.-Pellegrini,-Science-**347**,-1246501-(2015).-
[76] J.-Donnet-and-R.-Bansal,-Science-and-Technology,-Marcel-Dekker,-New-York-(1993).-
[77] A.-Peigney,-C.-Laurent,-E.-Flahaut,-R.-Bacsa,-and-A.-Rousset,-Carbon-**39**,-507-(2001).-
[78] Y.-Zhu,-S.-Murali,-M.-D.-Stoller,-K.-Ganesh,-W.-Cai,-P.-J.-Ferreira,-A.-Pirkle,-R.-M.-Wallace,-K.-A.-Cychosz,-M.-Thommes,-et-al.,-Science-**332**,-1537-(2011).-
[79] L.-Britnell,-R.-Ribeiro,-A.-Eckmann,-R.-Jalil,-B.-Belle,-A.-Mishchenko,-Y.-J.-Kim,-R.-Gorbachev,-T.-Georgiou,-S.-Morozov,-et-al.,-Science-**340**,-1311-(2013).-
[80] B.-Wang,-A.-Zhou,-F.-Liu,-J.-Cao,-L.-Wang,-and-Q.-Hu,-Journal-of-Advanced-Ceramics-**7**,-237-(2018).-
[81] C.-E.-Ren,-M.-Q.-Zhao,-T.-Makaryan,-J.-Halim,-M.-Boota,-S.-Kota,-B.-Anasori,-M.-W.-Barsoum,-and-Y.-Gogotsi,-ChemElectroChem-**3**,-689-(2016).-
[82] P.-Lian,-X.-Zhu,-S.-Liang,-Z.-Li,-W.-Yang,-and-H.-Wang,-Electrochimica-Acta-**55**,-3909-(2010).-
[83] J.-Hassoun,-F.-Bonaccorso,-M.-Agostini,-M.-Angelucci,-M.-G.-Betti,-R.-Cingolani,-M.-Gemmi,-C.-Mariani,-S.-Panero,-V.-Pellegrini,-et-al.,-Nano-Letters-**14**,-4901-(2014).-
[84] Z.-Fan,-J.-Yan,-L.-Zhi,-Q.-Zhang,-T.-Wei,-J.-Feng,-M.-Zhang,-W.-Qian,-and-F.-Wei,-Advanced-Materials-**22**,-3723-(2010).-
[85] Y.-DallAgnese,-P.-Rozier,-P.-L.-Taberna,-Y.-Gogotsi,-and-P.-Simon,-Journal-of-Power-Sources-**306**,-510-(2016).-
[86] Y.-Dall'Agnese,-M.-R.-Lukatskaya,-K.-M.-Cook,-P.-L.-Taberna,-Y.-Gogotsi,-and-P.-Simon,-Electrochemistry-Communications-**48**,-118-(2014).-
[87] B.-Anasori-and-Y.-Gogotsi,-*2D Metal Carbides and Nitrides (MXenes)* (Springer,-2019).-
[88] V.-Augustyn,-J.-Come,-M.-A.-Lowe,-J.-W.-Kim,-P.-L.-Taberna,-S.-H.-Tolbert,-H.-D.-Abruña,-P.-Simon,-and-B.-Dunn,-Nature-Materials-**12**,-518-(2013).-
[89] A.-A.-Lubimtsev,-P.-R.-Kent,-B.-G.-Sumpter,-and-P.-Ganesh,-Journal-of-Materials-Chemistry-A-**1**,-14951-(2013).-
[90] D.-Chen,-J.-H.-Wang,-T.-F.-Chou,-B.-Zhao,-M.-A.-El-Sayed,-and-M.-Liu,-Journal-of-the-American-Chemical-Society-**139**,-7071-(2017).-
[91] M.-Okubo,-A.-Sugahara,-S.-Kajiyama,-and-A.-Yamada,-Accounts-of-Chemical-Research-**51**,-591-(2018).-
[92] M.-Naguib,-J.-Come,-B.-Dyatkin,-V.-Presser,-P.-L.-Taberna,-P.-Simon,-M.-W.-Barsoum,-and-Y.-Gogotsi,-

Electrochemistry Communications **16**, 61 (2012).

[93] X. Wang, S. Kajiyama, H. Iinuma, E. Hosono, S. Oro, I. Moriguchi, M. Okubo, and A. Yamada, Nature Communications **6**, 1 (2015).

[94] M. Naguib, R. A. Adams, Y. Zhao, D. Zemlyanov, A. Varma, J. Nanda, and V. G. Pol, Chemical Communications **53**, 6883 (2017).

[95] J. Pang, R. G. Mendes, A. Bachmatiuk, L. Zhao, H. Q. Ta, T. Gemming, H. Liu, Z. Liu, and M. H. Rummeli, Chemical Society Reviews **48**, 72 (2019).

[96] J. Zhu, A. Chroneos, J. Eppinger, and U. Schwingenschlögl, Applied Materials Today **5**, 19 (2016).

[97] V. Shukla, N. K. Jena, S. R. Naqvi, W. Luo, and R. Ahuja, Nano Energy **58**, 877 (2019).

[98] C. J. Zhang, S.-H. Park, A. Seral-Ascaso, S. Barwich, N. McEvoy, C. S. Boland, J. N. Coleman, Y. Gogotsi, and V. Nicolosi, Nature Communications **10**, 1 (2019).

[99] Z. Ling, C. E. Ren, M.-Q. Zhao, J. Yang, J. M. Giammarco, J. Qiu, M. W. Barsoum, and Y. Gogotsi, Proceedings of the National Academy of Sciences **111**, 16676 (2014).

[100] P. Sobolčiak, A. Ali, M. K. Hassan, M. I. Helal, A. Tanvir, A. Popelka, M. A. Al-Maadeed, I. Krupa, and K. A. Mahmoud, PloS one **12**, e0183705 (2017).

[101] D. Wang, F. Li, R. Lian, J. Xu, D. Kan, Y. Liu, G. Chen, Y. Gogotsi, and Y. Wei, ACS Nano **13**, 11078 (2019).

[102] D. Li, X. Chen, P. Xiang, H. Du, and B. Xiao, Applied Surface Science **501**, 144221 (2020).

[103] M. Greaves, S. Barg, and M. A. Bissett, Batteries & Supercaps (2019).

[104] J.-M. Tarascon and M. Armand, in *Materials for sustainable energy: a collection of peer-reviewed research and review articles from Nature Publishing Group* (World Scientific, 2011), pp. 171–179.

[105] N. Nitta, F. Wu, J. T. Lee, and G. Yushin, Materials Today **18**, 252 (2015).

[106] T.-H. Park, J.-S. Yeo, M.-H. Seo, J. Miyawaki, I. Mochida, and S.-H. Yoon, Electrochimica Acta **93**, 236 (2013).

[107] A. Sarycheva, A. Polemi, Y. Liu, K. Dandekar, B. Anasori, and Y. Gogotsi, Science Advances **4**, eaau0920 (2018).

[108] E. Blanco, A. Rosenkranz, R. Espinoza-González, V. M. Fuenzalida, Z. Zhang, S. Suárez, and N. Escalona, Catalysis Communications **133**, 105833 (2020).

[109] Y. Gao, Y. Cao, H. Zhuo, X. Sun, Y. Gu, G. Zhuang, S. Deng, X. Zhong, Z. Wei, X. Li, et al., Catalysis Today **339**, 120 (2020).

[110] A. Shahzad, K. Rasool, W. Miran, M. Nawaz, J. Jang, K. A. Mahmoud, and D. S. Lee, ACS Sustainable Chemistry & Engineering **5**, 11481 (2017).

[111] A. Szuplewska, A. Rozmysłowska-Wojciechowska, S. Poźniak, T. Wojciechowski, M. Birowska, M. Popielski, M. Chudy, W. Ziemkowska, L. Chlubny, and D. Moszczyńska, Journal of Nanobiotechnology **17**, 1 (2019).

[112] A. Szuplewska, D. Kulpińska, A. Dybko, M. Chudy, A. M. Jastrzebska, A. Olszyna, and Z. Brzózka, Trends in Biotechnology (2019).

[113] G. Liu, J. Zou, Q. Tang, X. Yang, Y. Zhang, Q. Zhang, W. Huang, P. Chen, J. Shao, and X. Dong, ACS Applied Materials & Interfaces **9**, 40077 (2017).

[114] Z. Gan, H. Xu, and Y. Hao, Nanoscale **8**, 7794 (2016).

[115] Q. Xue, H. Zhang, M. Zhu, Z. Pei, H. Li, Z. Wang, Y. Huang, Y. Huang, Q. Deng, J. Zhou, et al., Advanced Materials **29**, 1604847 (2017).

[116] C. Dai, Y. Chen, X. Jing, L. Xiang, D. Yang, H. Lin, Z. Liu, X. Han, and R. Wu, ACS Nano **11**, 12696 (2017).

[117] H. Lin, Y. Wang, S. Gao, Y. Chen, and J. Shi, Advanced Materials **30**, 1703284 (2018).

[118] Z. Liu, H. Lin, M. Zhao, C. Dai, S. Zhang, W. Peng, and Y. Chen, Theranostics **8**, 1648 (2018).

[119] H. Liu, C. Duan, C. Yang, W. Shen, F. Wang, and Z. Zhu, Sensors and Actuators B: Chemical **218**, 60 (2015).

[120] R. Rakhi, P. Nayak, C. Xia, and H. N. Alshareef, Scientific Reports **6**, 1 (2016).

[121] E. S. Muckley, M. Naguib, H.-W. Wang, L. Vlcek, N. C. Osti, R. L. Sacci, X. Sang, R. R. Unocic, Y. Xie, M. Tyagi, et al., ACS Nano **11**, 11118 (2017).

[122] Y. Ma, N. Liu, L. Li, X. Hu, Z. Zou, J. Wang, S. Luo, and Y. Gao, Nature Communications **8**, 1207 (2017).

[123] K. Montazeri, M. Currie, L. Verger, P. Dianat, M. W. Barsoum, and B. Nabet, Advanced Materials **31**, 1903271 (2019).

[124] H. Tan, Q. Tao, I. Pande, S. Majumdar, F. Liu, Y. Zhou, P. O. Persson, J. Rosen, and S. van Dijken, Nature Communications **11**, 1 (2020).

[125] J. Bekaert, C. Sevik, and M. V. Milošević, Nanoscale **12**, 17354 (2020).

[126] S. Luo, S. P. Patole, S. Anwer, B. Li, O. Ogogotsi, V. Zahorodna, V. Balitskyi, K. Liao, et al., Nanotechnology (2020).

[127] S. Seyedin, J. Zhang, K. A. S. Usman, S. Qin, A. M. Glushenkov, E. R. S. Yanza, R. T. Jones, and J. M. Razal, Global Challenges **3**, 1900037 (2019).

[128] D. Horlait, S. C. Middleburgh, A. Chroneos, and W. E. Lee, Scientific Reports **6**, 18829 (2016).

[129] D. Horlait, S. Grasso, A. Chroneos, and W. E. Lee, Materials Research Letters **4**, 137 (2016).

[130] E. Zapata-Solvas, S.-R. G. Christopoulos, N. Ni, D. C. Parfitt, D. Horlait, M. E. Fitzpatrick, A. Chroneos, and W. E. Lee, Journal of the American Ceramic Society **100**, 1377 (2017).

[131] E. Zapata-Solvas, M. A. Hadi, D. Horlait, D. C. Parfitt, A. Thibaud, A. Chroneos, and W. E. Lee, Journal of the American Ceramic Society **100**, 3393 (2017).

[132] I. Ihsanullah, Nano-Micro Letters **12**, 1 (2020).

[133] J. Chen, Q. Huang, H. Huang, L. Mao, M. Liu, X. Zhang, and Y. Wei, Nanoscale **12**, 3574 (2020).

[134] L. Cheng, X. Wang, F. Gong, T. Liu, and Z. Liu, Advanced Materials **32**, 1902333 (2020).

[135] Y. Gogotsi and B. Anasori, *The rise of mxenes* (2019).

[136] J.-M. Tarascon, Nature chemistry **2**, 510 (2010).

[137] J. B. Goodenough and K.-S. Park, Journal of the American Chemical Society **135**, 1167 (2013).